Composites: Part B 61 (2014) 73–83

Contents lists available at ScienceDirect

Composites: Part B

journal homepage: www.elsevier.com/locate/compositesb

Nanofilled epoxy adhesive for structural aeronautic materials

U. Vietri [a,*], L. Guadagno [a], M. Raimondo [a], L. Vertuccio [a], K. Lafdi [b]

[a] Department of Industrial Engineering – DIIN, University of Salerno, Via Giovanni Paolo II, 132, 84084 Fisciano, SA, Italy
[b] University of Dayton, 300 College Park Dayton, OH 45440, USA

ARTICLE INFO

Article history:
Received 24 June 2013
Received in revised form 16 January 2014
Accepted 20 January 2014
Available online 27 January 2014

Keywords:
Polymer-matrix composites
A. Thermosetting resins
B. Adhesion
B. Mechanical properties

ABSTRACT

The aim of this work was to develop new adhesive formulations based on epoxy/nanostructured carbon forms. Different types of nanofillers were dispersed into an epoxy matrix for developing toughened epoxy paste aeronautic adhesives. The reinforced adhesives were used for bonding carbon nanofilled/epoxy composite adherents. Data were also compared to the results obtained both for the unfilled adhesive and/or adherents. Tensile butt joint, and single lap joint samples were prepared to measure mechanical strength and adhesion properties of the different joint configurations. The inclusion of carbon nanofillers inside the epoxy adhesive caused a significant improvement in the bond strength of the joints, changing the failure mode of joints in single lap joint shear tests. Significant change of the bonding performance was observed as the weight fraction of carbon nano-fillers increased from 1.37 to 5 wt/wt%. Adhesion between nano-reinforcements and adherents substrate was studied by means of Scanning Electron Microscopy.

1. Introduction

Adhesively bonded joints are increasing alternatives to mechanical joints in engineering applications and provide many advantages over conventional mechanical seal. To join such composite parts, polymer adhesives such as epoxies are commonly used. Using adhesive bonding for joining composite parts provides many advantages such as low cost, high strength to weight ratio, low stress concentration, fewer processing requirements and superior fatigue resistance and environmental resistance [1].

Adhesion between the polymer (composite) surface of adherents and polymeric adhesive substrate is suitably controlled by the chemical groups at or near the interface which lead to a better performance of bonded joint in their application [2]. Several papers have been published on the inclusion of nanostructured carbon forms inside epoxy adhesives in order to enhance the mechanical strength and toughness of the bonded joints [1,3–5]. Yu et al. (2009) studied the mechanical behavior and durability in humid environments of the aluminum joints bonded with an epoxy adhesive reinforced with multi-walled carbon nanotubes (MWCNTs) [3]. Likewise, Hsiao et al. (2003) studied the mechanical strength of epoxy/MWCNT reinforced adhesive to join carbon graphite fiber/epoxy composite adherents [1], while other researcher studied the adhesive properties of nanoreinforced epoxy adhesive using dissimilar joints composed of carbon fiber/epoxy laminate and aluminum alloy [4]. In any case, the presence of uniformly dispersed CNTs inside the adhesive paste was found to be able to increase bonding strength, Young's modulus as well as ultimate tensile strength of the adhesive. An improvement of CNT's reinforcement on fracture strength for adhesive joints was also observed between steel–composite interfaces and composite–composite interfaces [5]. MWCNTs embedded in the adhesive at a percentage of 1 wt% enhanced fracture toughness for both steel–composite and composite–composite adhesive joints. Adhesive performance of epoxy-based materials was investigated also considering the effects of inorganic nanoparticle inclusions on the adhesive strength of a hybrid sol–gel epoxy system used to joint, either aluminum substrate, and mild steel substrate [6]. The mechanical performance of different formulations was characterized by shear and tensile tests to define the influence of nanofillers on adhesive strength performance of the modified epoxy/hybrid sol–gel. The incorporation of a selected ratio of inorganic nanoparticles in the epoxy/sol–gel adhesive improves the adhesion performance between substrate surfaces. At the same time, it is well known in literature that one of the main predicted advantages related to the inclusion of conductive nanoparticles into epoxy resin is the improvement of its electrical behavior [7–11]. In fact, different types of carbon nanofillers are electrical conductor materials, which well dispersed in the matrix, can drastically increase electrical properties of epoxy based adhesives also using a very low percentage of nanofiller. This property is of special

* Corresponding author. Tel.: +39 089964019; fax: +39 089964057.
E-mail address: uvietri@unisa.it (U. Vietri).

http://dx.doi.org/10.1016/j.compositesb.2014.01.032
1359-8368/

relevance in the joint of electrical conductive substrates and makes adhesive epoxy/nanostructured carbon forms to become a promising new frontier in nanoreinforced adhesive for structural applications. The development of conductive epoxy adhesive to be used in the aeronautic field to join parts of primary structure is a current need with a view to optimizing efficiency of joints while preserving the conductivity of lightweight materials able to provide also in the joints good lightening protection [10,12,13]. The enhancement in different properties of epoxy-based materials and or/adhesives depend on numerous parameters, such as the chemical nature of nanofiller, adhesive and adherents, the applied surface treatment or the tested properties [14–16]. In the present study, we used as fillers heat-treated carbon nanofibers (CNFs) and exfoliated graphite. Heat-treated CNFs (at 2500 °C and 3000 °C) were chosen because they can impart higher conductivity than un-treated CNFs to the epoxy matrix. In particular, different papers dealing with the study on the effect of heat-treatment on CNFs report the beneficial effect on the electrical properties [16–18]; it is also possible to choice the best combination for improving electrical conductivity without to cause a decrease in the mechanical parameters of nanofilled resins [17,19]. In particular, for CNFs heat-treated at 2500 °C, the optimization of these properties were found [17]. The increase in the electrical conductivity consisting in a lower electrical percolation threshold (EPT) and a higher electrical conductivity beyond the EPT, with respect to the resin filled with untreated CNFs, was ascribed to the changes in morphology due to heat treatment (narrowing in the CNF diameter, increase in the length of the CNFs, less tendency to bend, absence of functional groups and then insulating layer on the CNF walls) [19]. Considering that this work is aimed at studying the properties of nanofilled adhesives for aeronautic materials able to hinder the insulating properties of epoxy resins, amount of nanofiller beyond EPT was chosen for all the analyzed nanofillers. In the case of the exfoliated graphite, a higher EPT was found than other nanofillers, then the lower concentration chosen in this paper was 3.7%. In addition, in this work, for the epoxy matrix of unfilled and nanofilled adhesives, a mixture of a tetrafunctional epoxy precursor with a reactive diluent (BDE) was used to facilitate the dispersion step of nanofilled adhesive. This is not a trivial problem especially when a nanofiller must be embedded in a specific resin for industrial applications. In fact, in the choice of the epoxy mixture it is necessary to consider that the structure of the resin strongly governs its chemical and some of the relevant physical properties. The number of reactive sites in the epoxy precursors controls the functionality directly acting on the cross-linking density and this, combined with the nature of hardener agent, the functionality, the stoichiometry and the curing cycle determines the final mechanical and thermal properties. In this case, we used a tetrafunctional epoxy precursor in combination with BDE. While the epoxy precursor is an already established reference material for aeronautic applications, its viscosity may hinder its usage for nanofilled adhesives. This mixture with BDE has never been used before as epoxy matrix for adhesive in aeronautic field.

An interesting aspect of this study is the different approach in preparing adhesive and adherents. In particular, adhesive and adherents were epoxy mixture and or nanofilled epoxy mixture with the same chemical composition in such a way as to obtain chemical interactions inside bonded joints and adherents of the same nature. In addition, a comparison between data detected for unfilled and filled epoxy formulations provided information on the effect of nanofiller into the adhesive formulations. A very relevant result of this work is the role of CNFs heat-treated at 2500 °C in the adhesive properties of the nanofilled formulations. In particular, epoxy formulations at loading rate of 1.3 wt/wt% have shown the best adhesive performance.

2. Experimental procedure

2.1. Materials and preparation

2.1.1. Epoxy resin

The epoxy matrix composite was prepared by mixing an epoxy precursor, tetraglycidyl methylene dianiline (TGMDA) (Epoxy equivalent weight 117–133 g/eq), with an epoxy reactive monomer 1,4-Butandioldiglycidylether (BDE) that acts as reactive diluent.

Epoxy precursor and reactive diluent, both containing an epoxy, were obtained by Sigma–Aldrich. The curing agent investigated for this study is 4,4′-diaminodiphenyl sulfone (DDS). This product was used at stoichiometric concentration with respect to oxirane rings.

2.1.2. Carbon nanofillers

Vapor-grown carbon nanofibers (CNFs) used in this study were produced at Applied Sciences Inc. and were from the Pyrograf III family. The CNFs used in this study are respectively labeled as PR25XTPS2500 and PR24XTHHT where XT indicates the debulked form of the both PR25 and PR24 family, PS indicates the grade produced by pyrolytically stripping the as-produced fiber to remove polyaromatic hydrocarbons from the fiber surface, 2500 is the temperature of the heat-treatment and HHT indicates the grade produced by heat-treating the as-produced carbon nanofiber to 3000 °C.

Exfoliated graphite (EG) is obtained by rapid heating of a graphite intercalation compound (GIC). Exfoliated graphite nanoparticles are composed of stacks of nanosheets that may vary from 4 to 40 nm as resulted from X-ray and SEM investigations.

2.1.3. Curing cycles

Adhesive formulations were cured by a two stage curing cycle: an initial step at moderate temperature (125 °C for 1 h) and the second one at higher temperature (180 °C for 3 h).

2.1.4. Preparation of adherents and adhesive

Tests were carried out on eight series of samples, each one characterized by different combination between adherents and adhesive formulations. The combinations are shown in Table 1. Two different nanofiller percentages were used in preparing the nanofilled formulations (1.3, 3.7 and 5 wt/wt%). These percentages were chosen to significantly improve mechanical behavior, and at same time, electrical conductivity. All the nanofilled adhesives, reached or were just beyond the EPT [9,13].

Epoxy blend (TGMDA and BDE) and DDS were mixed at 120 °C until complete hardener solubilization and then the mixture was cooled to 90 °C. CNFs (samples PR25XTPS2500 and HHT24) and EG (exfoliated graphite) were added and incorporated into the matrix at 90 °C by using an ultrasonication for 20 min. An ultrasonic device, Hielscher model UP200S (200 W, 24 kHz) was used. Such an incorporation method was chosen among other different techniques since it has proven to be very effective for other carbon nanostructured forms leading to the nanofilled resins characterized by the best mechanical and electrical properties [20].

Materials (unfilled and nanofilled epoxy mixture) were cured in two different mold geometry configurations made of Teflon (PTFE). The molds were designed by referring to existing international standard practice in the design of the specimens, in particular ASTM D 2094 and ASTM D 1002 were considered (Fig. 1a and b). In this way, a suitable configuration of specimens for tensile butt joint (referred to ASTM D 2095), and single lap joint (referred to ASTM D 3163) were respectively obtained to measure mechanical strength and adhesion properties in the different joint configurations.

Table 1
Summary of the prepared samples and experiments carried out in the present work.

Sample label	Adherent composition	Adhesive composition	Adhesive thickness (mm) in tensile butt joint	Adhesive thickness (mm) in lap joint shear
A	Epoxy mixture with 1.3 wt/wt% carbon nano-fibers HHT24	Epoxy mixture with 1.3 wt/wt% carbon nano-fibers HHT24	0.21	0.23
B	Epoxy with 1.3 wt/wt% carbon nano-fibers HHT24	Epoxy mixture	0.21	0.23
C	Epoxy mixture	Epoxy mixture with 1.3 wt/wt% carbon nano-fibers HHT24	0.15	0.25
D	Epoxy mixture	Epoxy mixture	0.19	0.26
E	Epoxy mixture	Epoxy mixture with 3.7 wt/wt% exfoliated-graphite	0.20	0.22
F	Epoxy mixture	Epoxy mixture with 5 wt/wt% carbon nanofibers PR-XT PS 2500	0.33	0.42
G	Epoxy mixture	Epoxy mixture with 1.3 wt/wt% carbon nanofibers PR-XT PS 2500	0.21	0.25
H	Epoxy mixture with 1.3 wt/wt% carbon nanofibers PR-XT PS 2500	Epoxy mixture with 1.3 wt/wt% carbon nanofibers PR-XT PS 2500	0.15	0.15

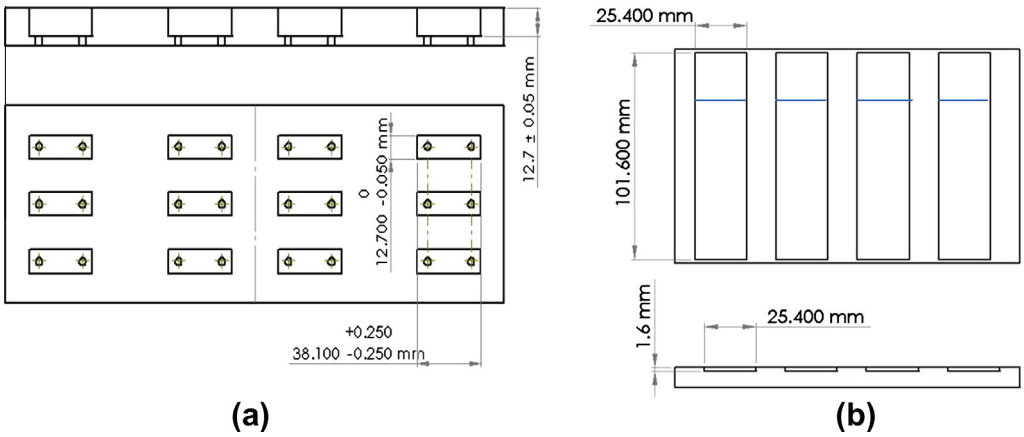

Fig. 1. (a) Schematic cavity geometry for tensile butt joint adherent and (b) schematic cavity geometry for lap joint shear adherent.

2.1.5. Joint configurations for mechanical testing

Figs. 2a and b and 3a and b show schematics of the tests set up used for the tensile and shear testing of the sample interfaces. These configurations were suitable selected as they are simple to make and assemble and involve different stress conditions mode to test the bonded joint between the adherent in axially and shear direction [21,22]. To assemble the adherents a very thin layer of adhesive was used (see Table 1). The thickness of the samples was measured using a digital caliper (accuracy 0.01 mm). For each type of combinations (adherents/adhesive) three different samples were tested and average measurement scatter turned out to be close to instrument accuracy. Before adhesive bonding, mechanical surface treatment (grit blasting) was performed for improving the adhesion between the parts.

Once the adhesive was placed between the overlap area, either the butt joint, than the single lap-joint samples were uniformly compressed in the overlapped adhesion area using two suitable devices based on clamping system (see Fig. 4a and b). They just apply weak pressure to allow the alignment of the adherents and no effects on the thickness of the adhesive layers are observed by measuring thickness of the adhesion layer after the curing process. The samples were then placed inside a convection oven followed by a curing cycle.

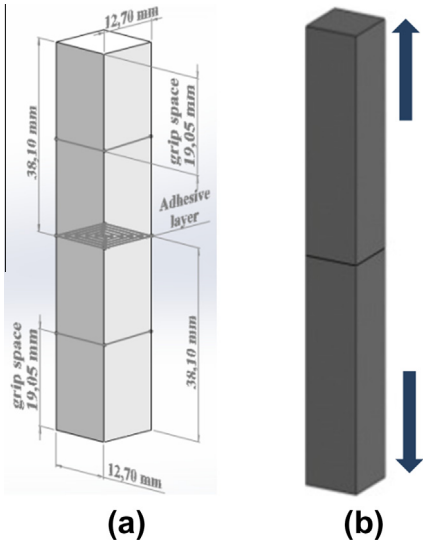

Fig. 2. (a) Schematic of the tensile butt joint strength test specimens (referred to ASTM D 2095) and (b) schematic of the butt joint (load direction).

2.2. Methods

2.2.1. Mechanical testing

Adhesive tests were carried out using an electro-hydraulic servo-controlled testing machine (Instron mod. 4301). Tensile and shear stress–strain characteristics, modulus of elasticity and ultimate tensile and shear strength of the nano-reinforced interface were measured. The loading was applied perpendicularly to the bonding plane, and the test procedures were carried out as ASTM D 2095 and ASTM D 3163 standard requirements. Tensile butt joint

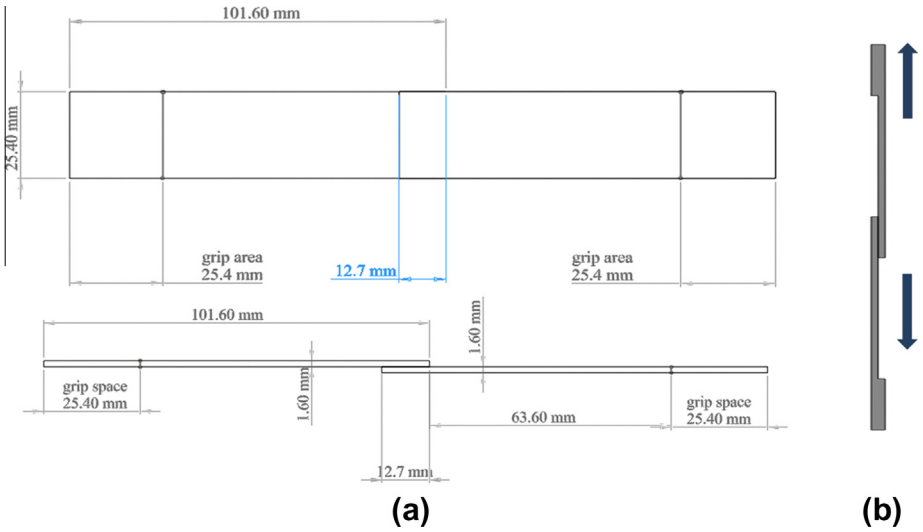

Fig. 3. (a) Schematic of the single lap-joint shear strength test specimens (referred to ASTM D 3163) and (b) schematic of the single lap-joint shear (load direction).

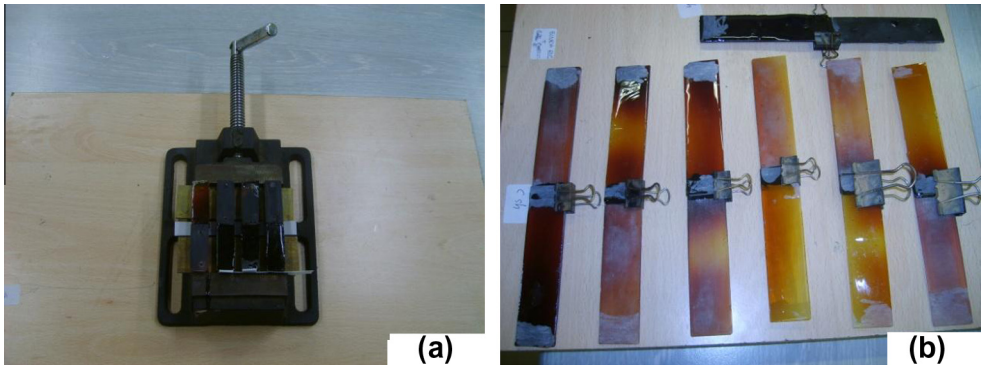

Fig. 4. (a) Assembly of the tensile butt joint specimens under uniform compression (before curing) and (b) assembly of the single lap joint shear specimens under uniform compression (before curing).

tests were performed applying a load to the specimens of 20 MPa/cm^{2}of bond area per min (3.1 kN/min), whereby, a load cell of 5 kN was necessary for the aim; whereas single lap joint shear tests were performed applying a load to the specimens of 9.7 MPa/cm^2 of overlapped area per min (3.1 kN/min), corresponding approximated by a free crosshead speed of 1.27 mm/min. It is worth noting that in the latter case, the load co-axiality was ensured using special adapters. In fact, the adherents were securely tightened to an adapter, which in turn was secured in the grips. This arrangement also ensured that no slip would take during the test (see Fig. 5b). Analogous to the tensile test, the loading train was vertically aligned prior to testing (see Fig. 5a). Several samples were tested for each set to determine average values of the mechanical strength of the joints. To calculate the tensile and shear strength of each sample, the maximum tensile load was divided by transversal bonded area, and by overlapping bonded area respectively; while to calculate the strain-to-failure values, the axial extension was divided by the gauge length of the specimens. A different approach was adopted in determining the elastic modulus. In fact, the tensile butt joint test can be used to estimate the adhesive's elastic modulus, but only after somewhat controversial corrections. The lap-shear test does not yield the elastic modulus, not even the shear modulus. Failure loads depend on specimen geometry and do not convey any additional information relative to failure stresses. It is well known in literature that tensile test on bulk specimens are clearly preferred for the aim [23]. Therefore, in addition to abovementioned adhesion tests, standardized samples referring to international standard ASTM D 638 (type V specimen configuration) were prepared and tested for measuring elastic modulus of the formulation joints (Fig. 5c). Several samples were tested for each set in tensile mode, by applying a loading rate of 1 mm/min. The Young's modulus was calculated as the slop of the stress–strain curve in the linear region.

Scanning Electron Microscopy (SEM) was carried out using FE-SEM (FE-SEM, mod. LEO 1525, Carl Zeiss SMT AG, Oberkochen, Germany) with the aim of studying the morphology of the detached zones. The fracture surfaces of the bonding areas were preliminary coated with a thin gold layer of 250 Å.

3. Results and discussion

Moduli, ultimate strengths and percentage strain-to-failure of the analyzed formulations are listed in Table 2. The samples are labeled as reported in Table 1 and the numbers are average values with the respective standard deviations.

Corresponding stress–strain characteristics, representative of the best performance of different samples, are displayed in Fig. 6a and b.

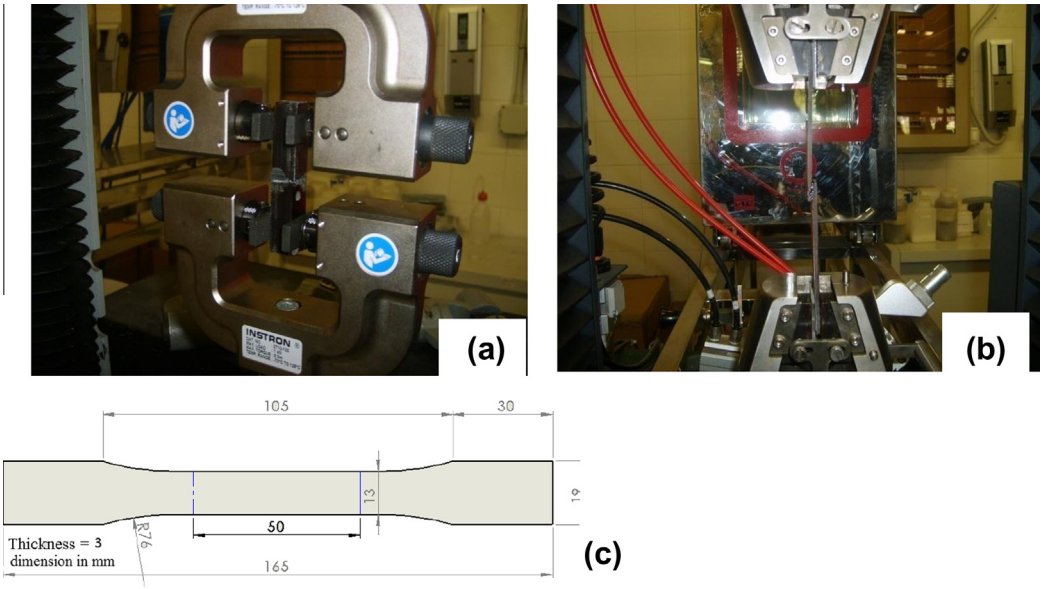

Fig. 5. (a) Tensile butt joint tests setup, (b) single lap-joint tests setup, and (c) geometry of the bulk adhesive test specimen.

Table 2
Summary of tensile and shear strength, and strain-to-failure values for all sets of composite specimens.

Sample label	Tensile strength of adhesives by axially loaded butt joints ASTM D 2095			Strength of adhesively bonded rigid plastic by lap-shear joints in shear by tension loading ASTM D 3163		
	Tensile strength @ break (MPa)	Strain percentage @ break (%)	Modulus (MPa)	Shear strength @ break (MPa)	Strain percentage @ break (%)	Modulus (MPa)
A	9.360 ± 0.073	5.278 ± 0.543	420.1 ± 8.23	6.430 ± 0.070	2.061 ± 0.011	417.37 ± 1.03
B	4.079 ± 1.200	1.303 ± 0.635	445.8 ± 7.43	3.843 ± 0.344	1.216 ± 0.020	418.07 ± 5.33
C	8.339 ± 0.800	3.391 ± 0.845	381.6 ± 12.21	4.693 ± 0.213	1.273 ± 0.120	391.5 ± 4.72
D	9.090 ± 1.650	3.797 ± 1.362	367.5 ± 7.54	**3.864 ± 0.123**	**1.109 ± 0.422**	**322.6 ± 10.71**
E	7.310 ± 0.235	2.777 ± 0.095	385.8 ± 9.65	**1.160 ± 0.047**	**0.801 ± 0.007**	**215.4 ± 12.37**
F	2.702 ± 0.257	0.956 ± 0.077	361.1 ± 11.36	2.276 ± 0.086	0.858 ± 0.002	245.7 ± 7.11
G	16.100 ± 0.620	5.517 ± 0.929	580.7 ± 17.72	5.422 ± 0.921	1.684 ± 0.021	423.9 ± 18.30
H	20.465 ± 1.135	5.326 ± 1.804	655.1 ± 27.74	5.612 ± 0.501	1.612 ± 0.106	571.4 ± 15.84

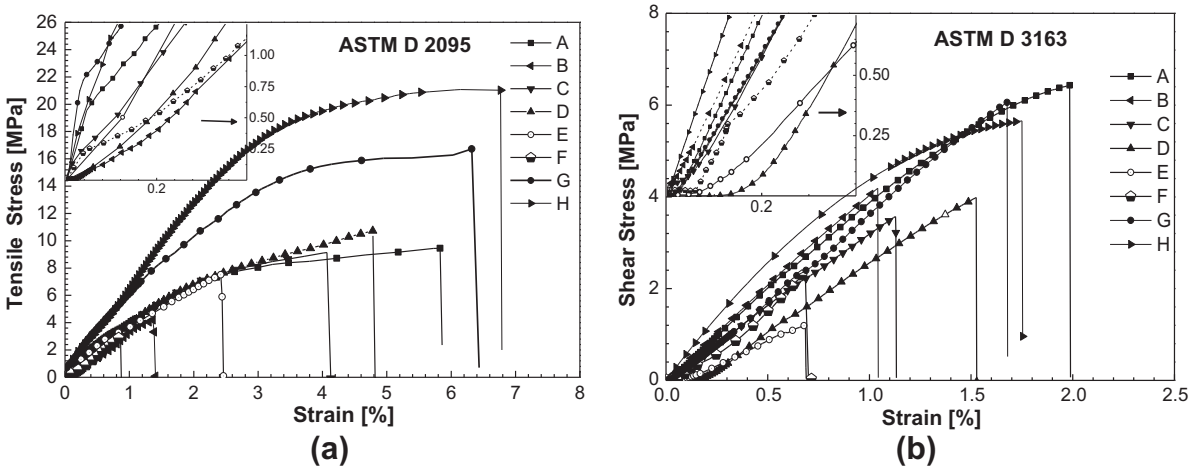

Fig. 6. (a) Stress–strain plot of bonded joints in tensile tests ASTM D 2095 and (b) stress–strain plot of bonded joint in lap-joint shear tests ASTM D 3163.

It is worth noting that data in Table 2 for samples D (adherent–epoxy mixture, adhesive–epoxy mixture) and E (adherent–epoxy mixture, adhesive–epoxy mixture filled with 3.7 wt/wt% exfoliated graphite), in lap joint shear configurations, (bold values), refer to samples failed in the bonded joint. A general view of these data highlights a strengthening of joint resistance as a result of

embedded nanofiller; even if the amount of nanofiller plays a very relevant role in determining this behavior. Samples A and H, which are made of nanofilled adhesive and nanofilled adherent with a percentage of 1.3 wt/wt% of CNFs, exhibit a very good adhesion behavior. In particular, sample H shows the best performance in the tensile strength parameter in butt joints configuration, whereas sample A exhibits the highest value of the same parameter in the lap-shear joints configuration. However, sample H, also in the case of lap-shear joints configuration, shows a significant strength, exceeded only sample A. Further, sample G, where only the adhesive past is loaded with 1.3% of CNFs (PR-XT PS 2500) shows a behavior in the adhesive performance better than samples B, D, E and F where the adhesive paste are unfilled (samples B and D) or filled with high percentage of nanofillers (samples E and F).

Considering all the results, we can certainly draw two important conclusions:

(a) the best adhesive behavior is obtained for samples filled with a low percentage CNFs (samples A and H) and with strong similarity in the chemical composition between adherents and adhesive (see samples A and H);
(b) in the performed tests (involving unfilled adherents and nanofilled adhesive) the best performance is obtained for low concentration of nanofiller (see samples F and G); in addition, CNFs heat-treated at 2500 °C show a better behavior than CNFs heat-treated at 3000 °C (see samples C and G).

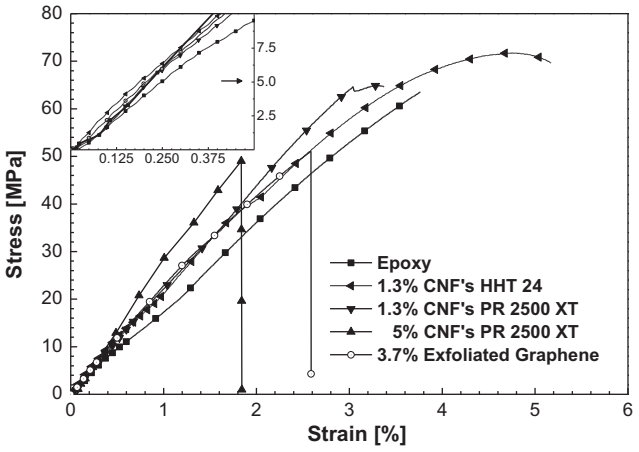

Fig. 7. Effect of nanofiller content on tensile stress–strain curve of adhesive formulations.

Table 3
Summary of tensile properties of epoxy modified adhesive.

Tensile properties of adhesives referred to ASTM D 638			
Specimen composition epoxy/wt/wt% nanofiller	Modulus (MPa)	Tensile strength (MPa)	Strain percentage (%)
1.3% CNF's HHT24	2464.4 ± 142.9	71.66 ± 6.63	4.75 ± 1.58
1.3% CNF's PR 2500 XT	2370.2 ± 25.41	64.87 ± 0.19	3.31 ± 0.28
5% CNF's PR 2500 XT	2845.3 ± 55.57	49.05 ± 3.14	1.83 ± 0.49
3.7% Exfoliated-graphene	2442.2 ± 52.36	51.08 ± 3.34	2.58 ± 1.28
Epoxy	2087.5 ± 15.57	63.56 ± 4.44	3.76 ± 4.60

The performed tests evidence the great potential of adhesive formulations as samples A and H in the field of structural adhesive materials. In fact, if the need arises, the structural adhesive can be tailored to replace the common adhesive with conductive adhesive to bond new nanofilled materials currently under investigation in the field of aeronautic and aerospace materials. Furthermore, market research indicates a more attractive price for the nanoparticles and many progress have been made in reducing difficulties related to the step of nanofiller dispersion. As already observed for different types of nanofillers in previous papers [4,24], also for carbon nanofibers, there is an optimum amount of nanofiller, which leads to significant improvement in mechanical behavior of the bonded joint. In fact, we can observed that, at higher nanofiller contents (i.e. 3.7 wt/wt% and 5 wt/wt%), the properties degrade to below the ones of the neat epoxy adhesive. Similar results were obtained in single lap joint shear tests.

Stress–strain curves and Young's modulus measured on bulk specimens are plotted in Fig. 7, whereas Young's modulus values are reported in Table 3. As already observed in literature [25] Young's modulus of the nanofilled epoxy formulations increases continuously with increasing nanofiller concentration, whereas the strength degrades with increasing loading rate of nanofillers.

3.1. Visual examination of failed joints

It is well known that it is the combination of adhesion and cohesive strength which determine bonding effectiveness. Cohesion is defined as the internal strength of an adhesive as a result of a variety of interactions within the adhesive. Adhesion is the bonding of one material to another, namely an adhesive to a substrate, due to a variety of possible interactions.

Generally, there are two possible mechanisms of failure, namely adhesive failure and cohesive failure. Adhesive failure is the interfacial failure between the adhesive and one of the adherents, which is indicative of a weak-boundary layer adhesion. On the other hand, cohesive failure occurs when the fracture results in a layer of adhesive remaining on both adherent surfaces, or, when the adherent fails before the adhesive with fracture almost contained in the adherent [21,26]. In our samples, failure in the bonded zone occurred for all the butt bonded joint samples tested by tensile

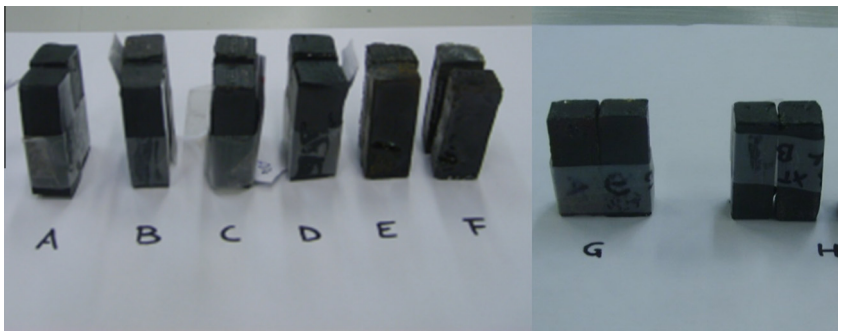

Fig. 8. Detail of failure of bonded joints occurred in butt joint tests.

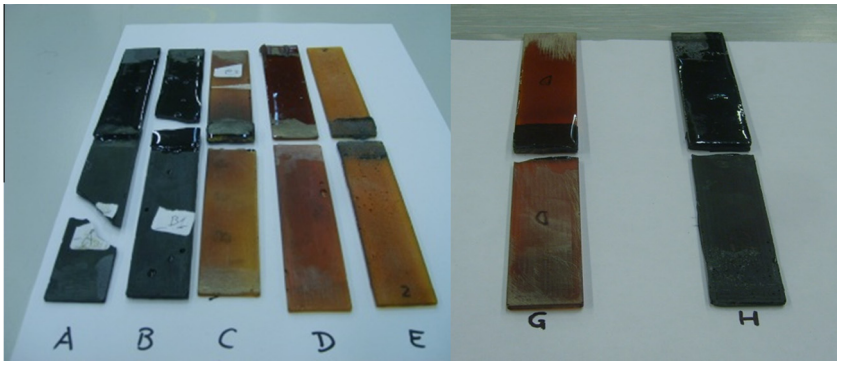

Fig. 9. Detail of failure of bonded joints occurred in lap joint shear tests.

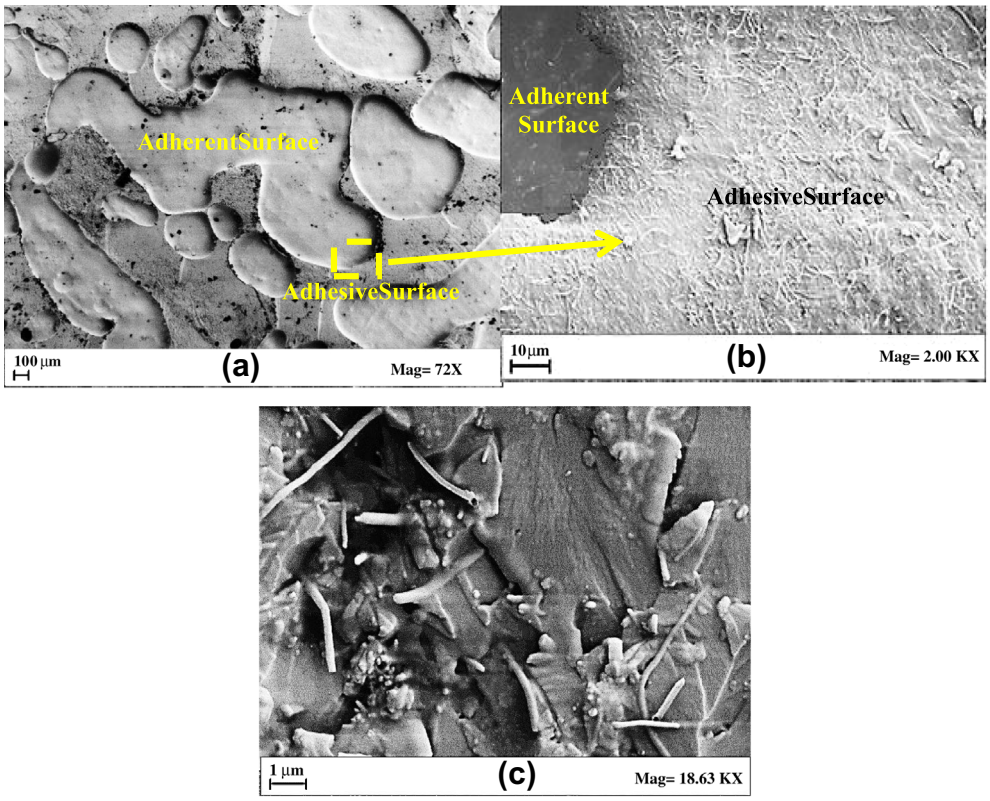

Fig. 10. (a and b) FE-SEM micrograph of fracture surface of the bonding areas-sample A failure in tensile test and (c) detail of magnifications of neighbor region.

mode (see Fig. 8). Different behavior was highlighted in single lap joint tests. In fact, sample D and E (Fig. 9), the adhesive breaks apart, and the failure occurred in the overlapped zone, although sample D exhibited high mechanical strength response (see Table 2). In other cases, inclusion of nanofiller in the adhesive paste, leads to no failure in the overlapped zone, because, the nanoreinforcement effectively transferred the load into the adherents, whether they were filled or unfilled. This last observation also highlights that a very important role in the joint behavior is also the nature of the interface adhesive/adherent, in fact also sample B shows a good behavior because the nanofillers interact in the interface zone.

Figs. 10–14 show SEM micrographs of fracture surface of butt joint tested in tensile mode. The inclusion of nano-reinforcement into the epoxy adhesive improves mechanical strength of the adhesive layer; it effectively transfer the external load to the adhesive layer containing nanofibers, and failure occurred also in the nanofibers (see Figs. 10b and 12b), which behave as the strongest part of the composite adhesive. In the same zones, few CNFs are even pulled out of the resin leaving micro and nanometric voids (see Figs. 10c–12b). In this regard, it is worth noting that no etching procedure was performed on the fracture surface before the morphological investigation. It is well known in the literature that the morphological investigation, by means of SEM investigations of nanofillers inside polymeric matrix, require pre-treatment of sample surfaces with etching procedure [27–30]. The simple fact of observing some nanofibers so clearly (see Figs. 10c and 12b) evidences that they have endured a load which has caused their detachment from the matrix. In the case of sample B, prepared by joining the nanofilled adherents with unfilled epoxy adhesive (see Fig. 11), no exposed CNF's are observable. In this case the failure of joint occurred at the epoxy along the bonding interface. This behavior might explain the lower values in the tensile strength of sample B with respect to the

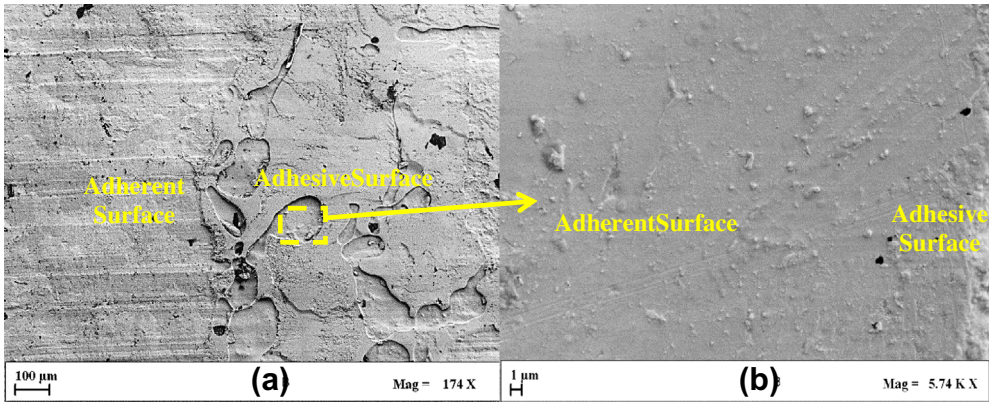

Fig. 11. (a) FE-SEM micrograph of fracture surfaces of the bonding areas-sample B failure in tensile test and (b) detail of magnifications of neighbor region.

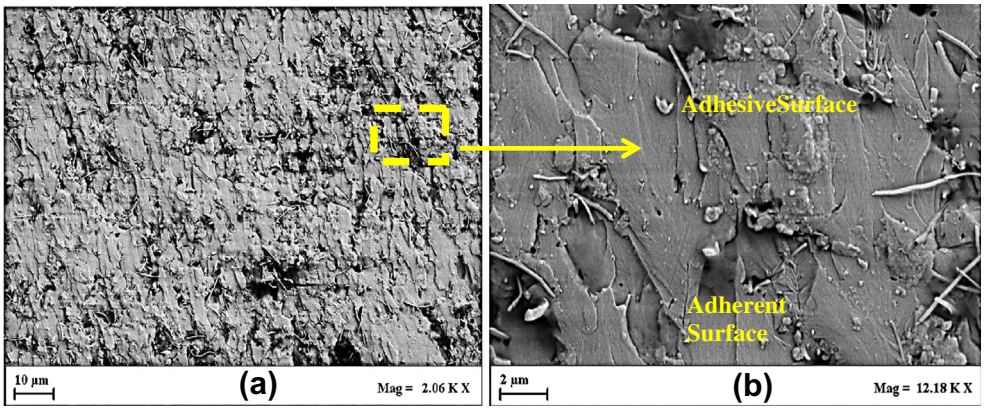

Fig. 12. (a) FE-SEM micrograph of fracture surfaces of the bonding areas-sample C failure in tensile test and (b) detail of magnifications of neighbor region.

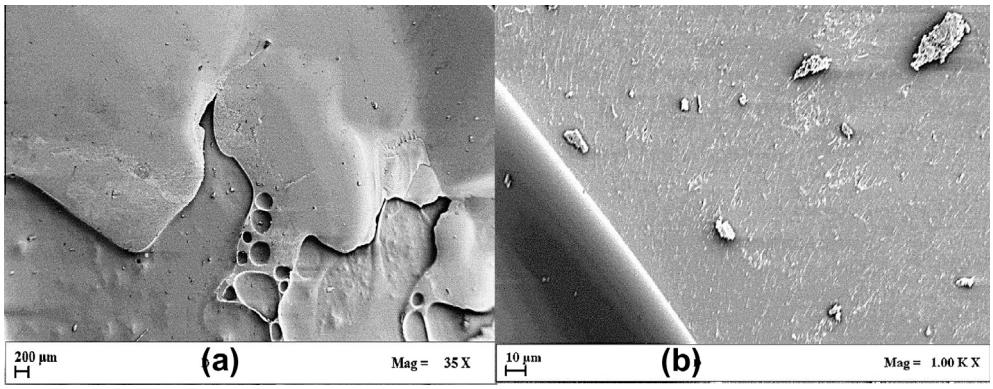

Fig. 13. (a) FE-SEM micrograph of fracture surfaces of the bonding areas-sample D failure in tensile test and (b) detail of magnifications of neighbor region.

previous sample or samples such as H, G and C samples. FE-SEM micrographs of bonding surface for unfilled joint (Fig. 13) show remnants of adhesive paste on unfilled surface which appear as a failure in the adhesive. Images on the fracture surfaces of sample E (see Fig. 14) show that the external load to which the joint is subjected, was supported by adhesive layer; in fact, the exfoliated graphene platelets are pulled out of the plan of interface. This occurrence confirms the same behavior observed for the fiber reinforced adhesive with a substantial difference: the high amount of exfoliated graphite platelets weakens the interaction between filler and matrix.

Fig. 15 shows the fracture surface of sample G: in this case two regions are clearly observed. In particular, dark zones (see zone A) corresponding to the failure between adhesive paste and adherent surface are distinguishable from the clear ones (see zone B) containing remnants of nanofilled adhesive. A magnification of the neighbor regions highlights the difference in phase compositions of the two different areas (see Fig. 16).

The dark ones differ from the others for the absence of CNFs; in fact, in the clear zones we can also see the distribution of the nanofibers and the effect of the tensile load on their interaction with the epoxy matrix. The influence of the tensile strength

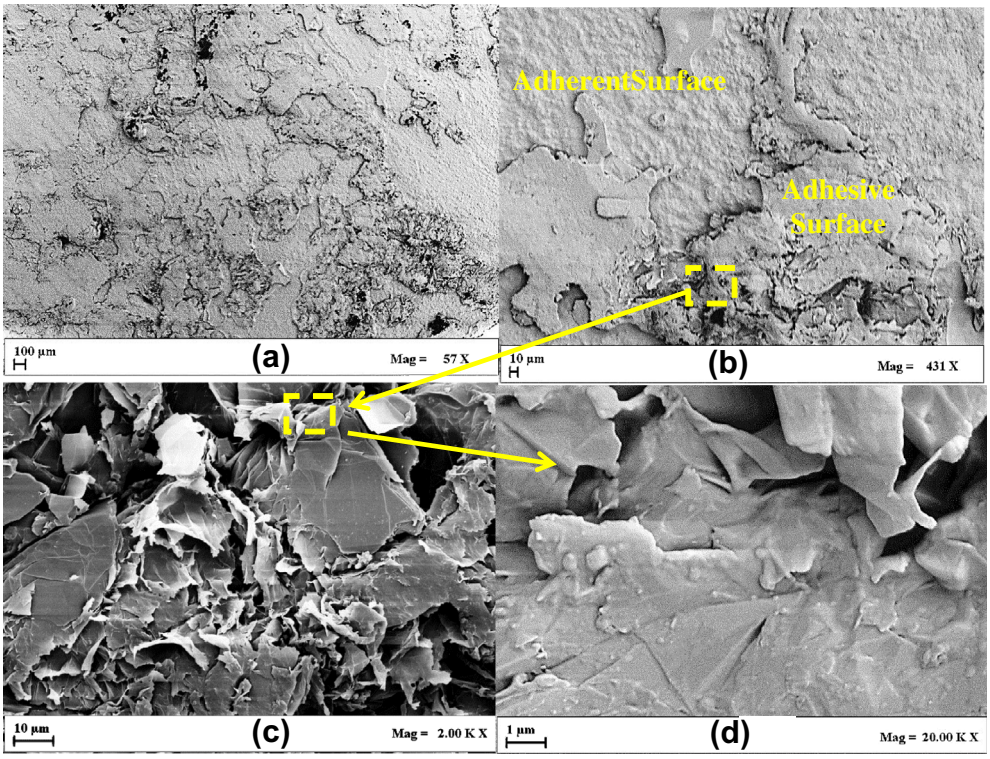

Fig. 14. (a and b) FE-SEM micrograph of fracture surfaces of the bonding areas-sample E failure in tensile test and (c and d) detail of magnifications of neighbor region.

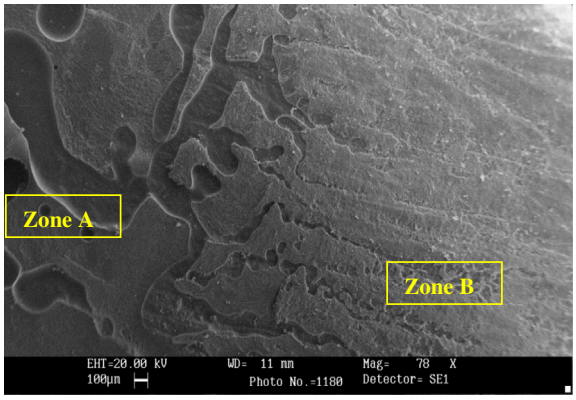

Fig. 15. FE-SEM micrograph of fracture surfaces of the bonding areas-sample G failure in butt joint test.

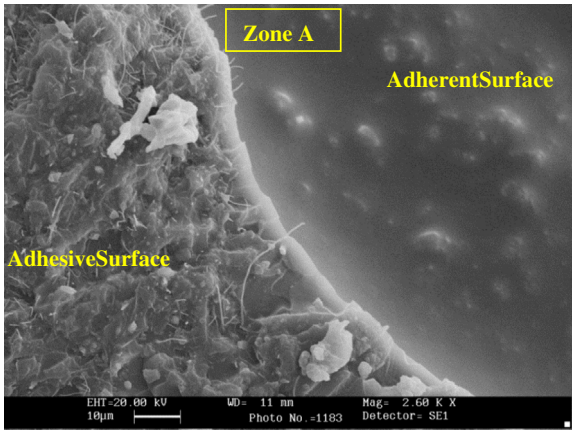

Fig. 16. FE-SEM magnification micrograph of the neighbor regions of fracture surfaces of the bonding areas-sample G failure in butt joint test (zone A).

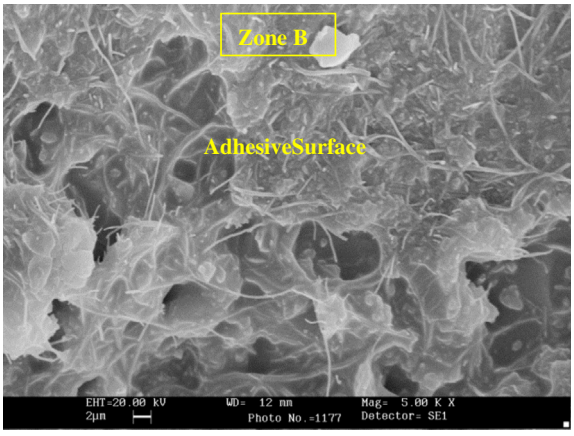

Fig. 17. FE-SEM magnification micrograph of the neighbor regions of fracture surfaces of the bonding areas-sample G failure in butt joint test (zone B).

experimented during the test causes a weakening of the interaction between CNF walls and epoxy matrix as evidenced from many nanofibers pulled out at the interface. In Fig. 17 of the same sample we can see the morphology of a large zone.

The different colors of the same morphological feature indicates a cohesive failure inside of the nanofilled adhesive paste. In this morphological analysis, a particular attention is focused on sample H which has shown the best adhesive behavior. Fig. 18 shows the fracture surface of sample H at low magnification.

The shades of gray seem to indicate that the majority of the surface is involved in a cohesive failure (zone B). This hypothesis is confirmed by other images at higher magnifications in the regions with clear tonality (see Fig. 19) where we can see an effect very similar to that of sample G (Fig. 17) in the regions where cohesive failures were observed.

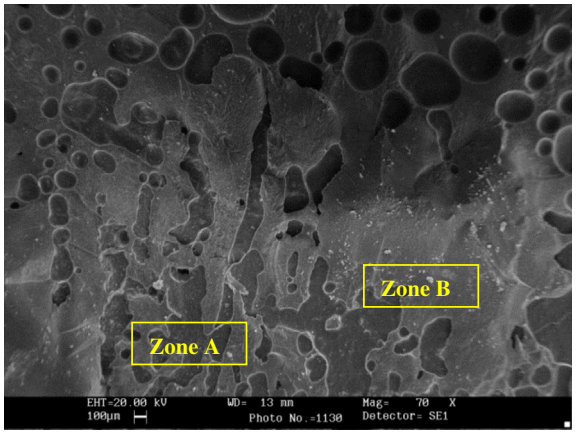

Fig. 18. FE-SEM micrograph of fracture surfaces of the bonding areas-sample H failure in butt joint test.

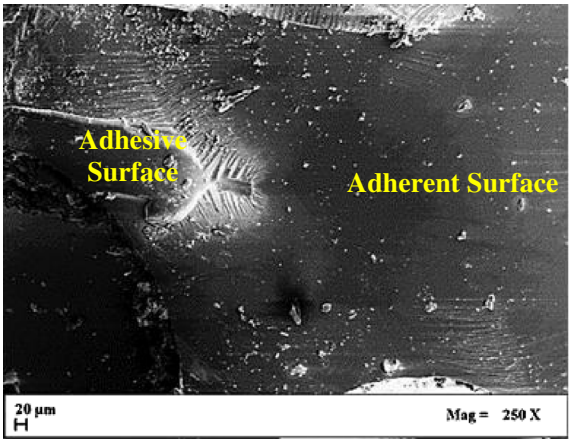

Fig. 21. FE-SEM micrograph of fracture surfaces of the bonding areas-sample D failure in lap joint shear test.

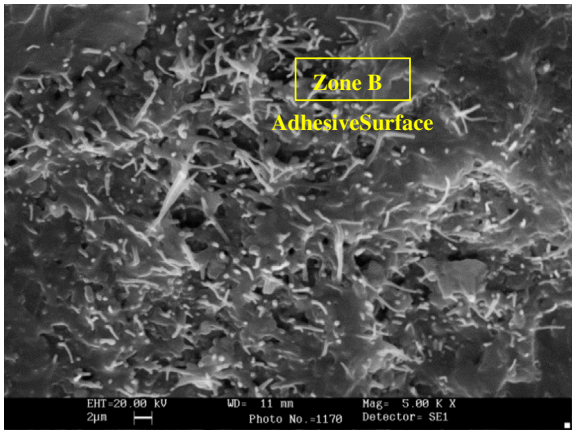

Fig. 19. FE-SEM micrograph of fracture surfaces of the bonding areas-Sample H failure in butt joint test.

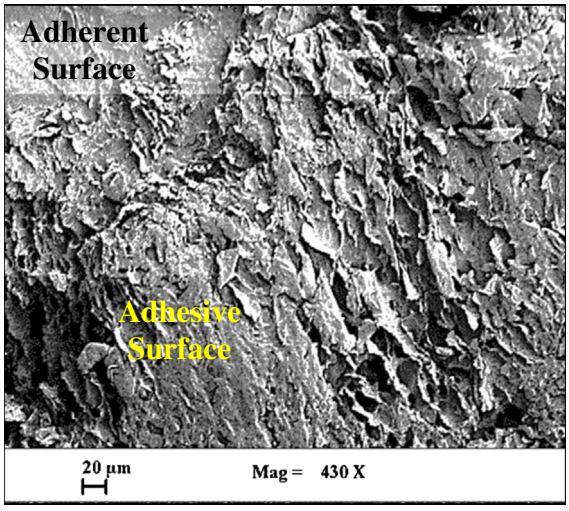

Fig. 22. FE-SEM micrograph of fracture surfaces of the bonding areas-sample E failure in lap joint shear test.

In Fig. 20 we show the fracture surface of neighbor regions (see zone A) in sample H. We can see that in some regions (at lower area percentage than the clear ones) the adhesive failure is observed; but in this case many CNFs are observable between the adherent surface and the adhesive paste. The CNFs seem detached from the resin showing a position of nanofibers subjected a strong tensile stress between the two faces. This last observation seems suggest that a stronger bond exists at the interface of sample H as a result of the strengthening effect resulting from the dispersed nanofillers and the strong compatibility between adherents and adhesive due to a very similar chemical composition.

Figs. 21 and 22 show the micrograph of the fracture surface of single lap joint tested in tensile mode refer to un-reinforced epoxy bonded joint (sample D), and for sample E. Either way, it was possible to observe a cohesive failure mechanism in bonded joint, and

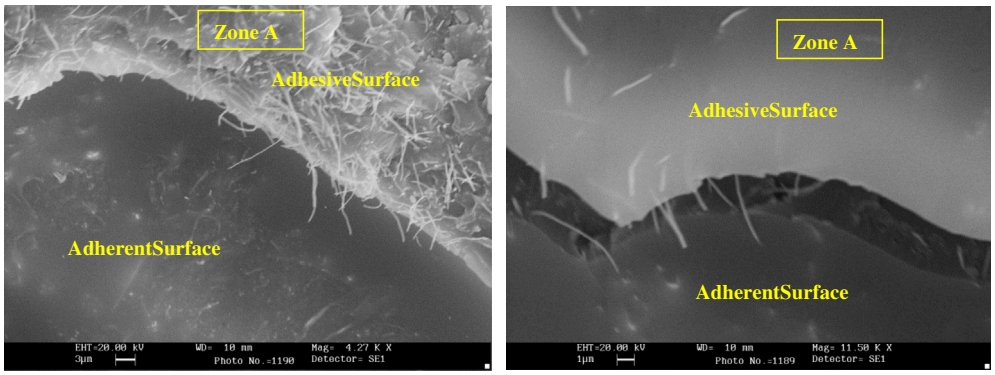

Fig. 20. FE-SEM magnification micrograph of fracture surfaces of the bonding areas-sample H failure in butt joint test (zone A).

in particular, Fig. 22 shows the presence of typical graphene platelets in adhesive paste which remained on the fracture surface.

From an overall view on the results, the reinforcement effect due to nanometric filler has proven to be very effective in improving the attractive interaction between adhesive formulations and adherent surfaces. If we observe the morphology of sample A and H, at higher magnification (Figs. 10b–20b), we can hypothesize that the network of nanomesh strongly increases the cumulative effect of Van der Waals interactions; their intensity is also amplified by the presence of the same nanofiller in the interface of adherent and epoxy adhesive. In the case of nanofiller or filler constitute of exfoliated graphite a negative effect is detected for the analyzed junctions. It is worth noting that in this last case the activities are in progress because in this paper, we have only used high nanofiller/filler concentration because our aim was to formulate a conductive epoxy adhesive and in the case of exfoliated graphite, the electrical percolation threshold was found for a higher percentage of filler [31,32].

4. Conclusions and remarks

The addition of carbon nanofillers into an epoxy adhesive formulation (studied for aeronautic application) caused a significant improvement in the bond strength of the joints, changing the failure mode of joints in single lap joint shear tests. The fracture of joints bonded with unfilled epoxy adhesive occurred at the epoxy along the bonding interface, and no significant damages were observed on the composite adherents. In contrast, the failure observed in nanoreinforced joints was cohesive in the adherents. The nanoreinforcing effectively transfer the load to in the adherents and the failure was in the composite. No difference in adhesive bonded joint were detectable in tensile tests of the analyzed samples. In any case, the most relevant enhancement in mechanical performance, were achieved by using lower nanofiller (1.3 wt/wt%) content in epoxy matrix, for both, adhesive and adherents, which formed the bonded joints. In the case of CNFs there is also the advantage with respect to CNTs of an easier production process mainly in the step of nanofiller dispersion inside the epoxy liquid adhesive which is a very difficult step before the curing process.

At higher nanofiller contents, (3.7 and 5 wt/wt%), adverse effects in bonded joints performance were observed. This occurrence might have resulted from aggregation and poor dispersion of the nanofiller into epoxy matrix, or also due to different nature between adherent surfaces and adhesive. Data shown in this paper highlighted the potentiality of adhesive nanofilled with CNF's to act as promising materials for joints in the new generation of aircraft materials.

Acknowledgements

This work was partly supported by POR CAMPANIA FSE 2007/2013, Asse IV e V, Reti di eccellenza FSE tra Università-Centri di ricerca-Imprese (Progetto MASTRI – linea di azione 1) and European Union Seventh Framework Programme FP7/2007-2013 under grant agreement no. 313978.

References

[1] Hsiao KT, Alms J, Advani SG. Use of epoxy/multiwalled carbon nanotubes as adhesives to join graphite fibre reinforced polymer composites. Nanotechnology 2003;14:791–3.
[2] Awaja F, Gilbert M, Kelly G, Foxa B, Pigram JP. Adhesion of polymers. Prog Polym Sci 2009;34:948–68.
[3] Yu S, Tong MN, Critchlow G. Wedge test of carbon-nanotube-reinforced epoxy adhesive joints. J Appl Polym Sci 2009;111:2957–62.
[4] Meguid SA, Sun Y. On the tensile and shear strength of nano-reinforced composite interfaces. Mater Des 2004;25:289–96.
[5] Burkholder Garrett L, Kwon Young W, Pollak Randall D. Effect of carbon nanotube reinforcement on fracture strength of composite adhesive joints. J Mater Sci 2011;46:3370–7.
[6] May M, Wang HM, Akid R. Effects of the addition of inorganic nanoparticles on the adhesive strength of a hybrid sol–gel epoxy system. Int J Adhes Adhes 2010;30:505–12.
[7] Gojny FH, Wichmann MHG, Fiedler B, Bauhofer W, Schulte K. Influence of nano codification on the mechanical and electrical properties of conventional fibre-reinforced composites. Compos Part A – Appl Sci Manuf 2005;36:1525–35.
[8] Wang T, Lei CH, Dalton AB, Creton C, Lin Y, Fernando KAS, et al. Waterborne nanocomposite pressure-sensitive adhesives with high tack energy, optical transparency, and electrical conductivity. Adv Mater 2006;18:2730–4.
[9] Nan CW, Shen Y, Ma Jing. Physical properties of composites near percolation. Annu Rev Mater Res 2010;51:40–131.
[10] Guadagno L, De Vivo B, Di Bartolomeo A, Lamberti P, Sorrentino A, Tucci V, et al. Effect of functionalization on the thermo-mechanical and electrical behavior of multi-wall carbon nanotube/epoxy composites. Carbon 2011;49:1919–30.
[11] De Vivo B, Guadagno L, Lamberti P, Raimondo M, Spinelli G, Tucci V, et al. Electrical properties of multi-walled carbon nanotube/tetrafunctional epoxy-amine composites. AIP Conf Proc 2012;1459:199–201.
[12] De Vivo B, Guadagno L, Lamberti P, Sorrentino A, Tucci V, Vertuccio L, et al. Comparison of the physical properties of epoxy-based composites filled with different types of carbon nanotubes for aeronautic applications. Adv Polym Technol 2012;31:205–18.
[13] Guadagno L, Raimondo M, Vittoria V, Lafdi K, De Vivo B, Lamberti P, Spinelli G, Tucci V. Role of the carbon nanofiber defects on the electrical properties of cnf-based composites. In: Menou A, et al., editors. ACMA Int Symp on Aircraft Materials (Fez, Maroc 09 May 2012); 2012. p. 55–6. ISBN: 9782953480429.
[14] Prolongo SG, Gude MR, Ureña A. In: Kumar A, editor. Nanoreinforced adhesives nanofibers; 2010. p. 438. InTech. ISBN 978-953-7619-86-2.
[15] Gude MR, Gòmez del Rìo T, Prolongo SG, Ureña A. Mode-I adhesive fracture energy of carbon fibre composite joints with nanoreinforced epoxy adhesives. Int J Adhes Adhes 2011;31:695–703.
[16] Lafdi K, Fox W, Matzek M, Yildiz E. Effect of carbon nanofiber–matrix adhesion on polymeric nanocomposite properties – Part II. J Nanomater 2008:8.
[17] Lafdi K, Fox W, Matzek M, Yildz E. Effect of carbon nano fiber heat treatment on physical properties of polymeric nanocomposites Part I. J Nanomater 2007:6.
[18] Endo M, Kim YA, Hayashi T, Yanagisawa T, Muramatsu H, Ezaka M, et al. Microstructural changes induced in "stacked cup" carbon nanofibers by heat treatment. Carbon 2003;41:1941–7.
[19] Guadagno L, Raimondo M, Vittoria V, Vertuccio V, Lafdi K, De Vivo B, et al. Role of the carbon nanofiber defects on the electrical and mechanical properties of CNF-based resins. Nanotechnology 2013;24:10.
[20] Guadagno L, Naddeo C, Vittoria V, Sorrentino A, Vertuccio L, Raimondo M, et al. Cure behavior and physical properties of epoxy resin – filled with multiwalled carbon nanotubes. J Nanosci Nanotechnol 2010;10(4):2686–93.
[21] Tsai MY, Morton J. An evaluation of analytical and numerical solutions to the single-lap joint. Int J Solids Struct 1994;31:2563–7.
[22] Messler RW. In: Troy, editor. Joining of advanced materials. New York (Boston): Butterworth-Heinemann; 1993. p. 560. ISBN 0750690089.
[23] Kim KS, Yoo JS, Yi YM, Kim CG. Failure mode and strength of uni-directional composite single lap bonded joints with different bonding methods. Compos Struct 2006;72:477–85.
[24] Saeed MB, Zhan MS. Adhesive strength of nano-size particles filled thermoplastic polyimides. Part-I: Multi-walled carbon nano-tubes (MWNT)-polyimide composite films. Int J Adhes Adhes 2007;27:306–18.
[25] Zhou Y, Pervin F, Rangari VK, Jeelani S. Fabrication and evaluation of carbon nano fiber filled carbon/epoxy composite. Mater Sci Eng A – Struct Mater Prop Microstruct Process. 2006;426:221–8.
[26] Suo Z. Fracture in thin films. In Prepared for encyclopedia of materials. Science and technology. Elsevier Science; 2001.
[27] Guadagno L, Vertuccio L, Sorrentino A, Raimondo M, Naddeo C, Vittoria V, et al. Mechanical and barrier properties of epoxy resin filled with multi-walled carbon nanotubes. Carbon 2009;47(10):2419–30.
[28] Guadagno L, Raimondo M, Naddeo C, Di Bartolomeo A, Lafdi K. Influence of multiwall carbon nanotubes on morphological and structural changes during UV irradiation of syndiotactic polypropylene films. J Polym Sci, Part B: Polym Phys 2012;50(14):963–75.
[29] De Vivo B, Lamberti P, Spinelli G, Tucci V, Guadagno L, Raimondo M, et al. Improvement of the electrical conductivity in multiphase epoxy-based MWCNT nanocomposites by means of an optimized clay content. Compos Sci Technol 2013;89:69–76.
[30] Guadagno L, Naddeo C, Raimondo M, Gorrasi G, Vittoria V. Effect of carbon nanotubes on the photo-oxidative durability of syndiotactic polypropylene. Polym Degrad Stab 2010;95(9):1614–26.
[31] Guadagno L, Raimondo M, Vittoria V, Vertuccio L, Lafdi K, De Vivo B, et al. Effect of conductive nanofiller structures on electrical properties of epoxy composite for aeronautic applications. In: 3rd International conference of engineering against failure (ICEAF III) Kos, Greece, 26–28 June 2013. p. 527–33. ISBN: 9789608810433.
[32] Guadagno L, Raimondo M, Vittoria V, Vertuccio L, Lafdi K, De Vivo B, et al. Electrical properties of CNFs/Epoxy-Amine Resin for aeronautic and aerospace applications. In: 3rd International conference of engineering against failure (ICEAF III) Kos, Greece, 26–28 June. p. 534–41. ISBN: 9789608810433.